Environ Geol (2007) 53:709–726
DOI 10.1007/s00254-007-0684-z

ORIGINAL ARTICLE

Investigations of subsurface flow constructed wetlands and associated geomaterial resources in the Akumal and Reforma regions, Quintana Roo, Mexico

Mark P. S. Krekeler · Pete Probst · Misha Samsonov · Cynthia M. Tselepis · William Bates · Lance E. Kearns · J. Barry Maynard

Received: 2 September 2006 / Accepted: 12 February 2007 / Published online: 8 March 2007

Abstract Subsurface flow constructed wetlands in the village of Akumal, Quintana Roo, Mexico were surveyed to determine the general status of the wetland systems and provide baseline information for long term monitoring and further study. Twenty subsurface flow wetlands were surveyed and common problems observed in the systems were overloading, poor plant cover, odor, and no secondary containment. Bulk mineral composition of aggregate from two subsurface flow constructed wetlands was determined to consist solely of calcite using bulk powder X-ray diffraction. Some soil structure is developed in the aggregate and aggregate levels in wetlands drop at an estimated rate between 3 and 10 cm/year for overloaded wetlands owing to dissolution. Mineral composition from fresh aggregate samples commonly is a mixture of calcite and aragonite. Trace amounts of Pb, Zn, Co, and Cr were observed in fresh aggregate. Coefficients of permeability (k) varied from 0.006 to 0.027 cm/s with an average values being 0.016 cm/s. Grain size analysis of fresh aggregate samples indicates there are unimodal and multimodal size distributions in the samples with modes in the coarse and fine sand being common. Investigations of other geologic media from the Reforma region indicate that a dolomite with minor amounts of Fe-oxide and palygorskite is abundant and may be a better aggregate source that the current materials used. A Ca-montmorillonite bed was identified in the Reforma region as well and this unit is suitable to serve as a clay liner to prevent leaks for new and existing wetland systems. These newly discovered geologic resources should aid in the improvement of subsurface flow constructed wetlands in the region. Although problems do exist in these wetlands with respect to design, these systems represent a successful implementation of constructed wetlands at a community level in developing regions.

Keywords Constructed wetlands · Mineralogy · Carbonate aggregate · Akumal

M. P. S. Krekeler (✉) · M. Samsonov · C. M. Tselepis
Department of Environmental Science and Policy,
George Mason University, Fairfax, VA 22030, USA
e-mail: mark.krekeler@gmail.com

P. Probst
Department of Earth and Environmental Sciences,
University of Illinois at Chicago,
845 W. Taylor St., Chicago, IL 60607, USA

W. Bates
United States Environmental Protection Agency, Region 5,
Water Division, 77 West Jackson Boulevard (WU-16J),
Chicago, IL 60604, USA

L. E. Kearns
Department of Geology and Environmental Sciences,
James Madison University, MSC 7703,
Harrisonburg, VA 22807, USA

J. B. Maynard
Department of Geology, University of Cincinnati,
Cincinnati, OH 45221-0013, USA

Introduction

Domestic wastewater treatment in the eastern Yucatan Peninsula is a growing concern both for human health reasons and because of the detrimental effect of untreated or poorly treated domestic wastewater on the environment (e.g., Sanchez-Gil et al. 2004; Herrera-Silvera et al. 2004). Furthermore coral reefs are declining on a global scale and sewage pollution is a major factor (Pennisi 2002; McKenna et al. 2001; Hughes and Connell 1999; Richmond 1993). The geologic environment of the eastern Yucatan

Peninsula is characterized by extensive karst aquifers that are particularly sensitive to waterborne pollution. These aquifer systems have extensive connectivity to the coastal marine environment and thus directly influence marine water quality impacting the coral reef. This hydrological relationship is important because the Meso-American reef is the second largest reef in the world and follows the entire eastern coast of the Yucatan peninsula. The overall health of the local Meso-American reef has been declining for several years (e.g., Shaw 1997) and much of this decline is attributed to untreated or poorly treated domestic wastewater effluent which enters the marine environment via karst aquifers. Wastewater effluent and sewage components are a common cause of coral reef deterioration worldwide (Pandolfi et al. 2005, 2003; Gardener et al. 2003; Pennisi 2002; McKenna et al., 2001; Hughes and Connell 1999; Richmond 1993). Furthermore human health concerns related to water quality are increasing in the region, especially for young children and the elderly as the karst aquifers serve as drinking water sources for populations in rural areas.

Domestic wastewater treatment options for the eastern Yucatan are limited and currently there are no large-scale, integrated wastewater treatment systems for the region. There are a few modern wastewater treatment plants that are in and near Cancun, yet most small communities south of Cancun do not have treatment plants or other wastewater treatment technologies. Some individual residents in some communities have septic tanks that function primarily as settling tanks. These systems do not effectively treat the sewage, but retain solids and discharge untreated wastewater into the environment. Solids are periodically pumped, usually at an expense of the equivalent of several hundred US dollars, and are commonly disposed of in the ecologically and hydrologically sensitive jungle.

Subsurface flow constructed wetlands are inexpensive alternative wastewater treatment technologies that are being utilized more commonly in developing regions (Okurut and van Bruggen 2000; Giraldo and Zárate 2000; Campbell and Ogden 1999; Stott et al. 1999; Nelson 1998; Panswad and Chavalparit, 1997; Denny 1997; Juwarkar et al. 1995). These technologies are complex engineered ecosystems involving hydrologic, biologic, and mineralogic processes to reduce wastewater volume and decrease or ideally eliminate the polluting components of wastewater (Wetzel 2001; Reed et al. 1995). Constructed wetlands have been in use for decades in North America and Europe (Kadlec and Knight 1996; Seidel 1976, 1966). These systems commonly consist of concrete boxes filled with aggregate and planted with vegetation and may have one or multiple cells (Kadlec and Knight 1996; Reed et al. 1995). Wastewater is piped into the subsurface of wetland cells where bacterial processes breakdown organic matter in wastewater and reduce BOD levels. The volume of wastewater introduced into the system is reduced by evapotranspiration.

Subsurface flow constructed wetlands have become an important wastewater treatment technology in the tourist-resort community of Akumal, located on the coast approximately 100 km south of Cancun (Fig. 1). During the early 1990s the community noticed a general decline in the health of the Meso-American reef, the primary economic attraction for the village. In the mid-1990s the Planetary Coral Reef Foundation (PCRF) sponsored the construction of several subsurface flow constructed wetlands (Fig. 2). These were engineered systems that were designed for specific loads (Nelson 1998) and were generally successful for their original design loads. This success served as an example for other individuals and businesses to utilize constructed wetlands in Akumal. Several constructed wetlands were installed since the mid-1990s. These wetlands were of variable design, and varied in the extent of engineering protocols followed during construction.

Only limited work on subsurface flow constructed wetlands in Akumal has been done. Whitney et al. (2003) conducted a preliminary evaluation of CEA wetland 1. This work examined the bulk properties of the wetland from a multi-day study. Their study focused on basic hydraulic characterization and COD analysis on this single wetland and did not conduct any detailed survey of any other wetlands in Akumal.

The goals of this investigation include documenting the general conditions and construction characteristics of the wetlands in Akumal to provide descriptive information useful for planning future work by scientists and engineers; investigating and determining key bulk geotechnical properties and the geologic nature of aggregate used in these systems; identifying better geologic resources to use in the wetland systems and to develop recommendations for better operating practices.

One aspect of these wetlands that has not received much attention is the nature and behavior of aggregate used in these systems. Although studies have investigated different substrates at a bulk level for performance purposes (i.e., Manios et al. 2002a, b), the mineralogy of aggregate is a commonly overlooked parameter in the study and design of constructed wetlands. Mineralogy of aggregate is often not investigated even though mineralogy can be a major influence on the physical and chemical processes operating in a given wetland. Water–mineral interaction may produce dissolution of aggregate. Different minerals have different stabilities and solubilities even if the physical–chemical conditions of the water have only minor fluctuations in in Eh and pH. Polymorphs, minerals that have the same chemistry but different crystal structures such as calcite

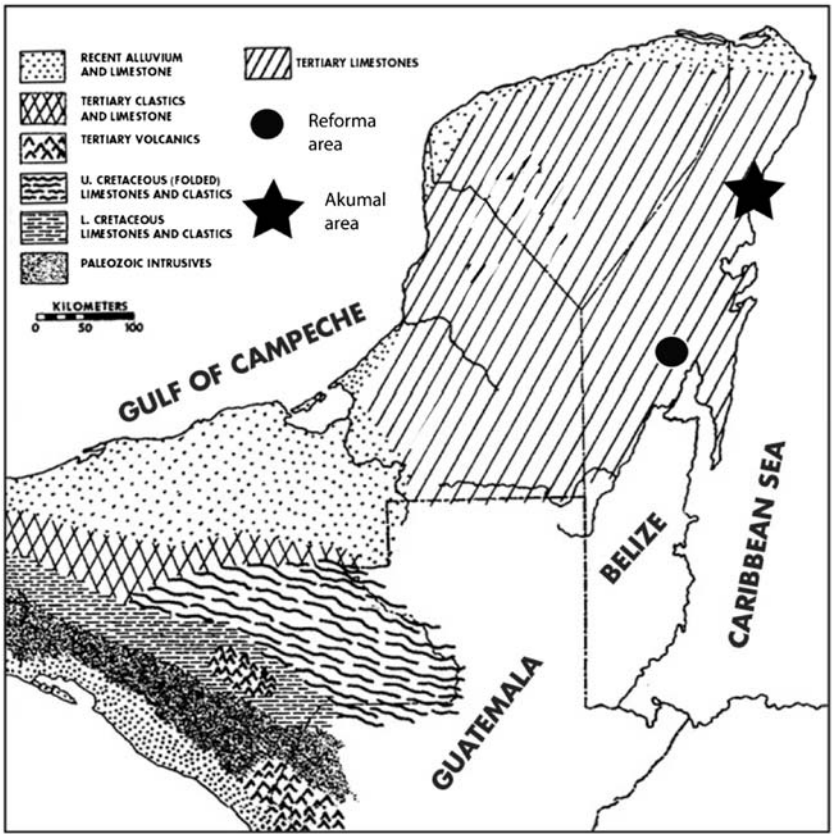

Fig. 1 Generalized geologic map adapted from Isphording (1984) of the Yucatan region with study localities identified

Fig. 2 **a** Irregularly shaped wetland with poor vegetation cover at La Bahia building. **b** One set of cells of the Las Casitas wetland, the largest in the area. Ferns are approximately 2 m in height. **c** CEA wetland 1 showing a diversity of plants, including palm trees, taro, and banana plants. **d** Wetland in south Akumal with abundant taro and other broad leaf vegetation

($CaCO_3$) and aragonite ($CaCO_3$) react and respond differently in the same geochemical environment. Mineralogy of aggregate may influence sorption behavior of a wetland system as different minerals have different crystal structures and have variation in properties of surface chemistry.

Limestone is the common aggregate utilized in all of the wetlands in the Akumal region. It is to date the only available aggregate. Bulk chemistry of the aggregate in some of the PCRF wetlands was characterized by Nelson (1998), however mineral identification and detailed studies of the mineralogy of any of the aggregate in the wetland systems in Akumal have not been performed. Limestone is a geologic material that can be complex and heterogeneous with respect to mineralogy. Source rocks for the aggregate

in the Akumal systems are believed to be Pleistocene or Tertiary in geologic age and thus there is the potential for both polymorphs of $CaCO_3$, calcite and aragonite to exist. Other carbonates that commonly occur in limestones and thus potentially occur in the wetland aggregates include high Mg-calcite, and dolomite (Boggs 1995; Tucker and Wright 1990; Klein and Hurlbut 1985). Calcite, aragonite, and dolomite have been reported in Pleistocene limestones in the eastern Yucatan (Ward and Brady 1979; Brady 1974) and high Mg-calcite is a common mineral found in many limestones. Non-carbonate minerals that commonly occur in limestone or are commonly associated with limestone include sulfate minerals such as gypsum and anhydrite, oxide minerals such as hematite, and goethite, and phyllosilicate minerals such as illite and chlorite (Moore and Reynolds 1997; Boggs 1995; Tucker and Wright 1990; Klein and Hurlbut 1985). All of these minerals have the potential to react with wastewater and thus knowing whether they are present in the aggregate in the Akumal subsurface flow constructed wetlands is important for understanding processes operating in the wetlands.

Materials and methods

A survey was conducted of 20 subsurface flow constructed wetlands in Akumal during the Fall of 2003. The number of cells, control boxes, holding tanks, areas, and estimated plant cover were determined for each system. Volume of aggregate, and when possible the water level within the wetlands were determined.

Samples

Aggregate was sampled from two subsurface flow constructed wetlands in Akumal, Quintana Roo, Mexico. Aggregate was taken from a PCRF wetland designated CEA wetland 1, which has been in operation since 1996, and has an apparent loss of gravel between 30 and 35 cm. One profile of aggregate from CEA wetland 1 was inspected in detail and measurements of aggregate were made. Four aggregate samples were also taken from a wetland constructed in 2001 for Las Casitas residences. Ten samples of fresh aggregate were collected from newly dumped piles that were to be used in wetland systems.

Coefficients of hydraulic conductivity (k) of materials were determined using a falling head permeameter. For fresh aggregate changes in permeability were monitored with time and final permeability measurements were taken when values stabilized, often after 2–3 liters of flow had been introduced. Grain size distribution of samples was determined using a full set of 8-inch mechanical sieves.

Alternative geologic media from the Reforma region (N 18°45.866′ and W 88°29.488′) was also investigated (Fig. 1). Clay material was obtained from an outcrop in an unnamed creek where a secondary access road, adjacent to the main road and bridge, leads to the outcrop in the creek where the unit is exposed approximately 10–40 cm above the water level (Fig. 3). Underlying the clay unit is a dolomitic limestone bed. The contact with this lower unit is gradational with 3–5 cm of nodular dolomitic limestone pebbles composing 15–25% of this material. The remaining overlying material is approximately >>95% clay. A sharp undulating upper contact separates the clay unit from an overlying dolomitic limestone. A quarry approximately 200 m west of the clay locality contains dolomite unit (Fig. 3). Samples of exposed units being mined for road aggregate were obtained.

Five samples of the clay unit were exchanged with 0.1 N Mg^{2+} solution five times and then washed with deionized water. The <2 μm size fraction (upper 5 cm of suspension collected after a 2.5 h settling time) was collected and centrifuged. Clay material was removed and smear mounts were prepared on zero-background quartz slide mounts. Slides were analyzed under air-dry, ethylene glycol-exchanged, and glycerol-exchanged conditions. X-ray diffraction scans were made using a Seimens D-5000 using Cu $K\alpha_2$ radiation operated at 40 kV and 25 ma. Step size for the scans was 0.02° 2θ with a count time of 1 s per step. For transmission electron microscopy (TEM), the <2 μm size fraction was collected from suspensions that had not been exchanged with Mg^{2+}, and was diluted with deionized water for selected samples. Grain mounts were prepared by placing a drop of the suspension on 3 mm Cu grids with holey carbon film. Grids were allowed to dry overnight. TEM investigation was conducted using a JEOL JEM-3010 microscope operated at 300 kV, equipped with a Noran EDS system and Gatan CCD image capture system.

All wetland aggregate samples used for X-ray diffraction analysis were obtained from approximately 10 cm below water level. X-ray diffraction was conducted on crushed powders of all aggregate samples. Samples were scanned from 20 to 55° 2θ at 0.02° steps using a count time of 1 s, or similar ranges. Aragonite was identified based on PDF #00-041-1475. The (111) reflection is most intense for aragonite and $d_{(111)}$ = ~0.338 nm. Calcite was identified using PDF# 00-047-1743. The (104) reflection is most intense for calcite and $d_{(104)}$ = ~0.303 nm. Mineral identifications were confirmed with the computer program Jade 6.0. Dolomite was identified using PDF#36-0426. The (104) reflection is most intense for dolomite and $d_{(104)}$ = ~0.288 nm.

SEM investigation was obtained using a LEO 1430VP Scanning Electron Microscope using a standard tungsten filament. Energy dispersive spectroscopy (EDS) analyses

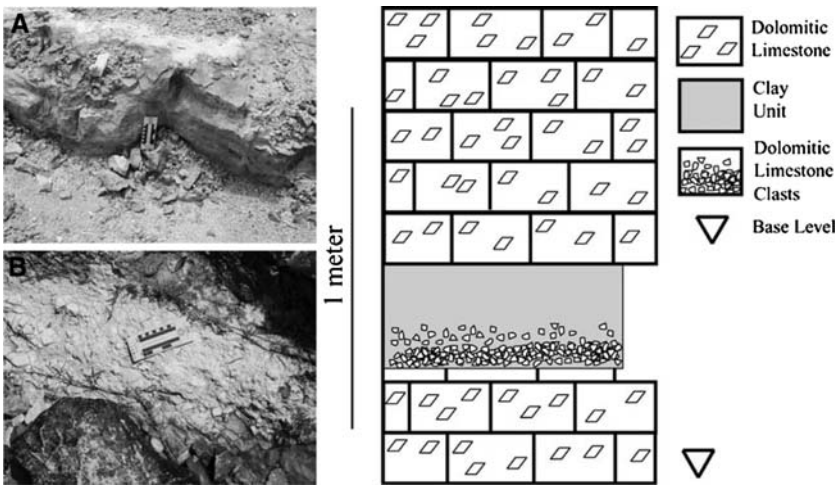

Fig. 3 Field photographs and stratigraphic column of Reforma materials. **a** shows an image of a bed of dolomite currently mined for road aggregate. **b** shows the Clay unit investigated. The stratigraphic column is a composite of the clay unit exposure in the stream

were obtained using an Oxford, Inc., light element energy dispersive spectrometer in conjunction with the SEM. Element analyses and presentation utilized ''*INCA*'' software, a product of Oxford, Inc.

Results

Setting and construction characteristics of constructed wetlands

Survey of the subsurface flow constructed wetlands in Akumal reveals a range in size and condition. Representative photographs of some of wetland systems in Akumal are presented in Fig. 2 and survey data are summarized in Table 1.

The physical status of the constructed wetlands in Akumal were generally good. Most of the constructed wetlands were built using concrete block and mortar. One wetland was constructed using fossil coral and mortar. All of the wetlands are structurally sound based on visual inspections. In no instance was cracking or spalling present. However, the status of the bottom of the wetland systems remains undetermined. No apparent secondary containment features such as geotextile or other low permeability linings were observed in any wetland system in Akumal.

The number of cells per system and the geometry of cells in the constructed wetlands in Akumal is variable, but is dominated by rectangular layouts which are used in 70% of the systems. The remaining 30% of the systems have irregular shapes, with two ''L-shaped'' wetlands, one rhombohedral, one circular-polygonal, and one figure-eight-shaped wetland. Wetland systems in Akumal consist of single and multiple cell systems with 65% being single cell systems and the remaining 35% being multiple cell systems. Commonly both cells in two cell systems have approximately the same dimensions and gravel and water levels are commonly 5–20 cm offset between cells. All of the multiple cell systems are two cell systems with the exception of the Las Casitas system that has a total of four cells but has two tandem wetlands. Areas of single cell wetlands vary between 4.00 and 41.97 m^2 with an average area of 16.19 m^2 and areas of multiple cell systems vary from 21.41 to 351.81 m^2 with an average area of 100.74 m^2. The largest wetland is the multiple cell system at Las Casitas.

Control boxes, piping, and cleanouts are an integral part of constructed wetland systems because they allow regular maintenance, allow access for sampling and in some instances may permit retrofit modifications. Control boxes are in 65% of the wetlands and some systems have multiple control boxes. Not all control boxes are readily accessible as some are overgrown or placed in unusual positions within the wetlands. Cleanouts have been placed in 45% of the wetlands. All visible piping in the systems is 4 in. white PVC. Piping where exposed is in good condition and most clean outs are easily accessible. Clean outs are particularly important for these wetlands because non-degradable debris occasionally enters these systems. One common problem that occurs is the introduction of various plastic bags into the systems. These are occasionally flushed down toilets and accumulate to block portions of the systems, particularly the spreader pipes.

Water levels were observed near the surface and also occasionally above the aggregate levels of the wetlands in 35% of the surveyed systems. Water levels may be above that of the stand-pipe control owing to pore occlusion. This is most commonly observed where there is small angular aggregate (<1 cm) high organic matter, or rapid increases or pulses of flow associated with high use periods. Wastewater near the surface of the aggregates can contribute to odor and can promote fungal growth.

Table 1 Survey data of wetland systems compiled from this investigation

Wetland	Geometry	No. of cells	No. of clean outs	No. of control boxes	No. of holding tanks	Total area (m^2)	Aggregate volume (m^3)	Agg. size (cm)	Pipe	Water depth	Odor	Fractures	Mulched ant	Cov
Las Casitas	Rectangular	4	8	2	2	351.8	240	1–3.5	4 in. PVC	1–2 cm	Weak	None	No	95
CEA wetland 1	Rectangular	2	0	2	1	87.6	55	1–5	4 in. PVC	2–8 cm	Strong	None	No	65
CEA wetland 2	Rectangular	2	0	2	1	53.1	44	1–5	4 in. PVC	5 cm	Moderate	None	No	75
Coral wetland	Rectangular	2	0	0	1	21.4	8	3–5	4 in. PVC	nd	None	None	No	45
First signed wetland	Rectangular	1	0	0	1	14.0	7	2–3	4 in. PVC	nd	None	None	Self	100
First ''L'' shaped	Equant ''L'' shape	1	2	2	1	22.0	17	2–4	4 in. PVC	18–24 cm	None	None	No	65
La Bahia	Rhombohedral	1	2	1	5	42.0	35	2–4	4 in. PVC	2–3 cm	Moderate	None	No	15
S. Mi Casa del Mar	Rectangular	1	0	1	1	12.7	9	1–3	4 in. PVC	7 cm	None	None	No	80
Casa del Mar 1	Rectangular wall	1	0	0	1	4.0	1	Soil	4 in. PVC	nd	None	None	No	100
Casa del Mar 2	Equant ''L'' shape	1	0	2	1	18.9	17	1–3	4 in. PVC	5 cm	Weak	None	No	75
Casa Carib*	Equant ''L'' shape	1	2	1	1	16.8	14	2–4	4 in. PVC	nd	Weak	None	No	80
Casa Zama	Rectangular	1	2	1	1	23.1	22	1–3	4 in. PVC	nd	Moderate	None	No	80
North of Casa Zama	Rectangular	1	4	0	0	19.3	16	1–2	4 in. PVC	nd	None	None	No	75
Vista del Mar Norte	Semi square	2	0	0	0	47.5	43	2–3	4 in. PVC	nd	None	None	No	85
Near La Bahia	Rectangular	2	4	2	0	96.7	59	2–4	4 in. PVC	4–5''	Moderate	None	sparse	50
Akumal Real estate	Rectangular	1	2	1	1	4.7	4	2–3	4 in. PVC	nd	None	None	No	90
Casa de los Suenos	Rectangular	1	0	1	2	6.0	6	Soil	4 in. PVC	nd	None	None	No	85
Casa Christensen*	Figure 8	1	0	0	1	13.9	14	3–4	4 in. PVC	nd	None	None	self	95
Que Onda	Circular Polygonal	2	0	0	1	47.1	56	2–3	4 in. PVC	nd	Moderate	None	No	95
West of Que Onda	Rectangular	1	4	1	1	13.0	11	2–3	4 in. PVC	nd	None	None	No	25

Vegetation data is in percentages. Aggregate size is range of observed clasts. ''nd'' could not be determined

Odor is a common problem in 45% of the wetlands and may be a qualitative indicator of poor performance. Weak and moderate odor occurs in eight wetlands and strong odor occurs in one wetland. Odor is most common in systems that are overloaded, or have a degraded control box seal, and systems that have water levels very near the surface of the aggregate. The CEA wetland 1 system is very much overloaded and has a very strong odor. One feature of a wetland that reduces odor is mulching. No wetlands are purposely mulched, however three systems are self-mulched from accumulation of dead vegetation.

Most wetlands have moderate plant cover that varies from 15 to 100% with an average cover of 74%. This plant cover consists of trees, shrubs, ferns, and leafy plants. Trees are commonly palms and are present in 55% of the wetlands

Investigations of existing aggregate

All of the constructed wetlands in Akumal have limestone aggregate. This aggregate is angular to sub-angular crushed limestone and most commonly is 2–3 cm in diameter. Some aggregate is smaller, for example the Las Casitas wetlands have very angular aggregate that is commonly <1 cm in diameter. Much of the aggregate in the wetlands show apparent corrosion that indicates dissolution is occurring in most systems. Further evidence of dissolution is that aggregate levels are commonly several centimeters to as much as 60 cm below their supposed original fill levels, being even with the walls.

Aggregate levels in some of the wetlands of Akumal were at lower levels than the bounding walls indicating that aggregate levels had dropped. Interviews with persons involved in the construction of both PCRF and other wetlands indicated that most wetlands were filled with aggregate to levels at or very near the tops of the walls. Levels of aggregate in older wetlands were several centimeters lower than the tops of walls commonly between 15 and 35 cm lower, and in one instance 60 cm lower whereas younger wetlands seemed to have minimal lowering of aggregate levels commonly only 5 cm lower. Levels of aggregate in PCRF supported wetlands have lowered 15–60 cm over the past 6 years owing to mineral dissolution.

In both CEA wetland 1 and the Las Casitas wetlands there is crude soil structure developed in the aggregates. Three horizons can be identified in these wetlands and commonly in other wetlands in the Akumal region. A representative section of aggregate from CEA wetland 1 was taken and described (Fig. 4). The upper horizon A (0–10 cm depth) has apparent oxide coatings, a great deal of organic material and has well developed root material. The underlying horizon B (10–20 cm depth) commonly has less

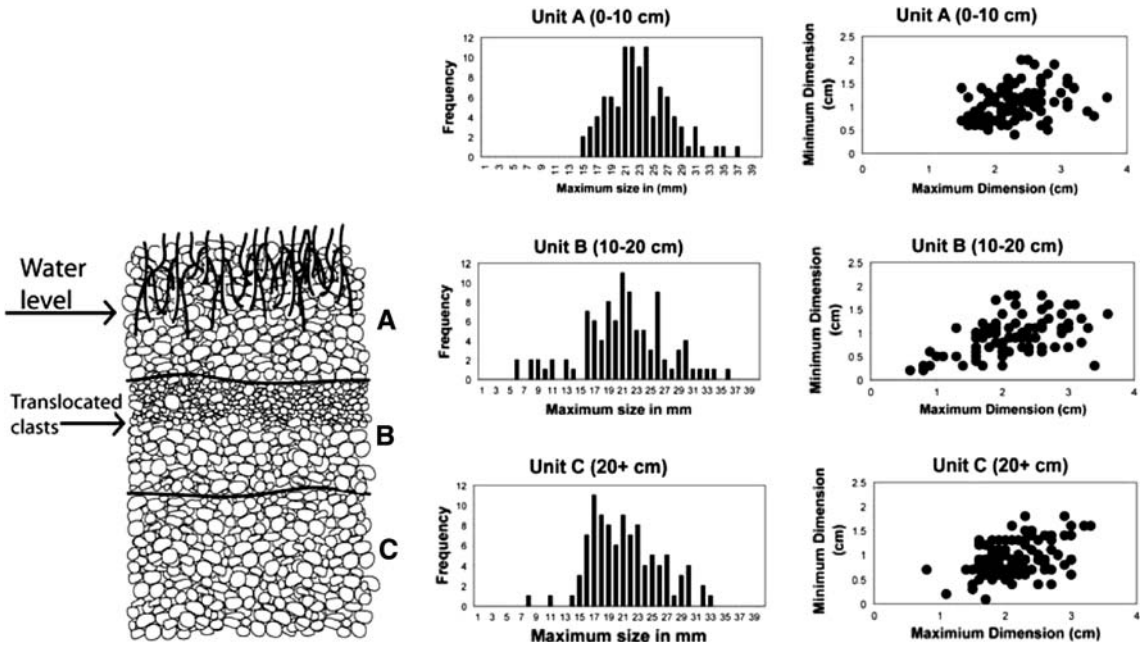

Fig. 4 Illustration showing three horizons within the aggregate of CEA wetland 1. Units A and B are approximately 10 cm thick and unit C is 20+ cm thick. Water level at time of sampling is labeled. Unit B has an accumulation of small clasts in the upper 4–6 cm that have been translocated from unit A. Adjacent column shows histograms of the three units shown graphically in drawing. Unit B is enriched in fine clasts derived from unit A. Far right column shows plots of maximum length versus minimum length of the three units shown graphically in drawing. Diagram shows there is large variation in shape, but all clasts plot to the right of the 1:1 ratio and are elongate in shape. This is likely an artifact of crushing

oxide coatings and less organic material than that of horizon A. Smaller aggregate clasts (<1 cm) have been translocated to horizon B from horizon A, mimicking natural soil forming processes. Horizon C (20+ cm depth) is parent material aggregate which has organic material dispersed both on clast surfaces and in pore space. All but the upper 5 cm of the section was saturated with wastewater. One hundred clasts from each horizon were measured to determine size characteristics (Fig. 4). Histograms of clast size show that clasts have a unimodal distribution and vary in size from 6 to 37 mm. Histograms of horizon B show that finer clasts have accumulated in this unit. Plots of minimum and maximum dimensions of clasts show a range of variability and show that clasts are elongated in shape (Fig. 4).

Aggregate from the Las Casitas constructed wetland is angular to sub-rounded, and frequently shows evidence for dissolution in the surface textures of clasts. Control aggregate samples are commonly angular, and are approximately 2–3 cm in average diameter. Samples of quarry limestone are poorly to moderately cemented, friable, and have an estimated porosity of 10–15% in hand samples.

Powder X-ray diffraction indicates that the mineralogy of all four aggregate samples from the Las Casitas constructed wetland was composed of calcite only and all ten aggregate samples from the CEA constructed wetland were also composed of calcite only (Fig. 5). No measurable quantities of aragonite or other minerals were detected in either set of wetland aggregate samples.

Investigations of fresh aggregate

The finer gravel used in the Las Casitas wetland and found in dump piles was determined to be likely more suitable for use in wetlands than the coarse gravel owing to lower permeability expected of the materials. Accordingly we investigated ten samples in detail.

X-ray diffraction on fresh aggregate samples indicated that calcite and aragonite are the dominant minerals present (Fig. 6). Five samples (AKS4, AKS5, AKS6, AKS8, AKS9) had appreciable amounts of aragonite where the other samples (AKS1, AKS2, AKS3, AKS7, AKS10) consisted of calcite. Estimates of the percentage of aragonite when present in the samples varies from approximately 10 to 60% based on simple peak comparison of area.

SEM investigation of selected samples of fresh aggregate indicates a wide spectrum of shapes and sizes of calcium carbonate particles (Fig. 7). Particles commonly vary from 0.5 to 9 μm in diameter. Pores are commonly irregular in shape and compose approximately 5–15% of the rock. Little textural variation was observed between samples.

Grain size analysis indicates there are unimodal and multimodal size distributions in the samples (Fig. 8). Five samples had unimodal distributions with common modes being at 3.35 or 4.00 mm. Multimodal samples were bimodal or trimodal with common modes being at 3.35 mm, 2.80 mm, 2.36 mm, 1.41 mm, 600 μm, 250 μm and 125 μm.

Coefficients of permeability (k) were measured for fresh aggregate samples and varied from 0.006 to 0.027 cm/s with an average values being 0.016 cm/s (Table 2). Observed values were compared to three methods for estimating k based on grain size distribution. The method of Alyamani and Sen (1993) was used because this method considers both grain size and sorting. The traditional methods of Hazen (1911) and the method of Sheperd

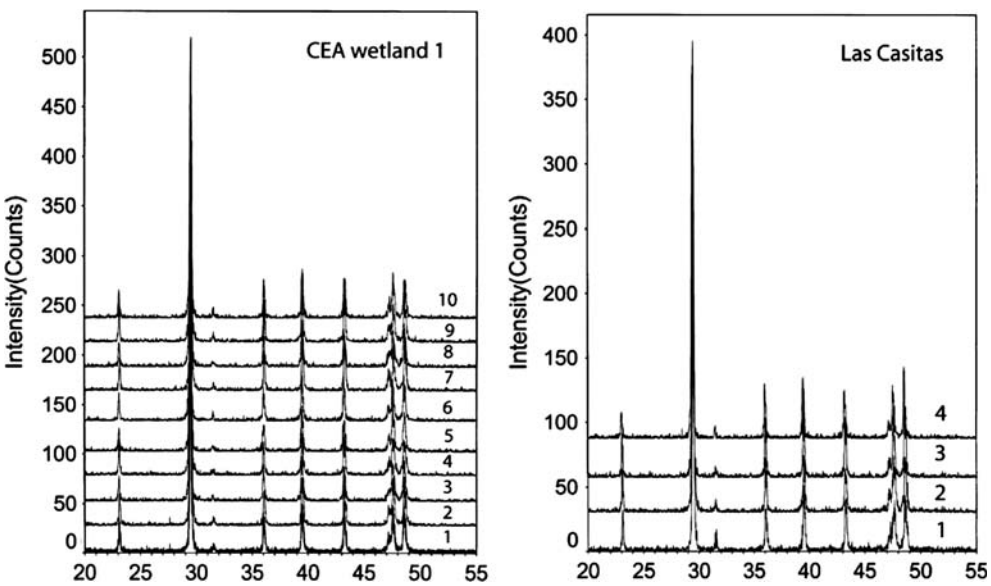

Fig. 5 X-ray diffraction patterns from CEA wetland 1 and Las Casitas wetlands samples consist solely of calcite

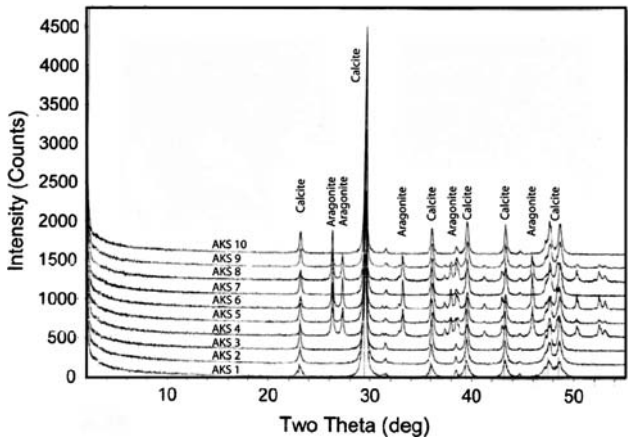

Fig. 6 X-ray diffraction patterns from fresh aggregate samples AKS1–AKS10 with major peaks of respective minerals labeled

(1989) were used. All units were converted to cm/s. The method of Sheperd (1989) was the closest to the observed values using parameters for immature sediments where

$$K = Cd^{j}$$

and $C = 100$, d = average grain size, and $j = 1.5$. This method still overestimated K by approximately 0.02 cm/s, over twice the average value observed. The Hazen (1911) method however overestimated K by approximately two orders of magnitude and the method of Alyamani and Sen (1993) overestimated K by approximately one order of magnitude.

Bulk XRF investigation of minor and trace metal concentrations in the fresh aggregate samples indicates that some heavy metals are present at ppm concentrations (Table 3). These are Pb (3–4 ppm), Zn (3–4 ppm), Co (1–11 ppm) and Cr (2–7 ppm). Concentrations of Mo, Cu, and Ni are all below detection limits (<1 ppm). V (b.d.–56 ppm) and Ti (0.003–0.035 wt% TiO_2) are also present. Minor elements commonly incorporated into marine biogenic calcium carbonate polymorphs are present in concentrations consistent with Plesitocene or Holocene limestones and are Ba (4–15 ppm), Sr (541–4,004 ppm), U (0.13–1.37 ppm) and Th (b.d.–1.1 ppm). Elements commonly associated with igneous, metamorphic or siliciclastic rocks show low concentrations as expected and are Nb (1.0–2.1 ppm), Zr (~36 ppm), and Y(8–10 ppm).

Investigation of geomatierals found in the Reforma region

Clay unit

Powder X-ray diffraction patterns of oriented samples indicate that smectite is the dominant mineral in the clay unit (Fig. 9). Small ~0.715 and ~0.35 nm peaks occur in all samples and these peaks are interpreted as kaolinite. Mg-air dried treatment shows a *d*-spacing for (001) reflections that varies between 1.50 and 1.60 nm. Mg-ethlyene glycol treatment shows *d*-spacings for (001) between 1.70 and 1.73 nm. Mg-glycerol exchange shows *d*-spacings for (001) to be slightly larger than those for Mg-ethlyene glycol treatment being between 1.78 and 1.88 nm. The expansion of (001) from approximately 1.50–1.60 nm in the Mg-air dried treatment to 1.70–1.73 nm in the Mg-ethlyene glycol treatment along with the Mg-glycerol

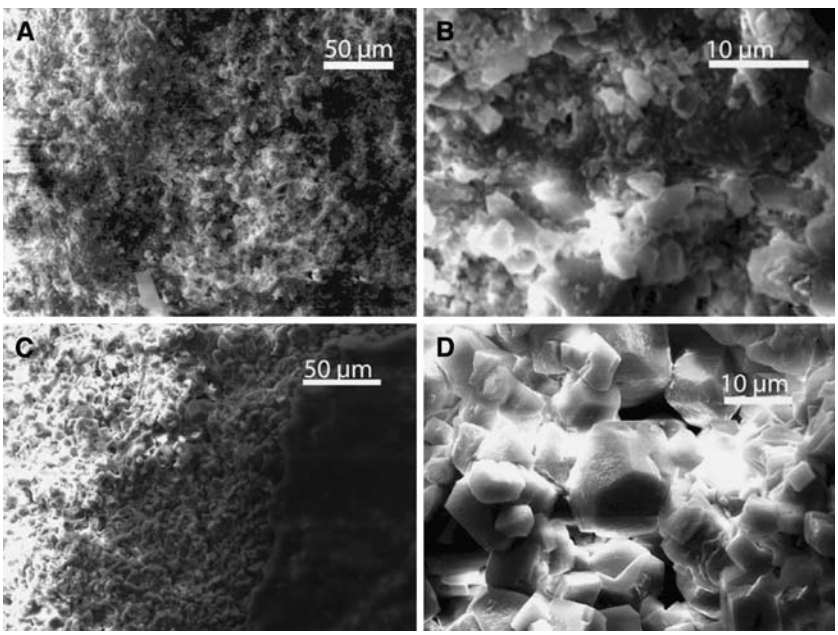

Fig. 7 SEM images. **a** and **b** are representative images of fresh aggregate samples showing irregular grain and pore shape. **c** and **d** are representative images of the dolomite from Reforma showing uniform size distribution and euhedral crystals

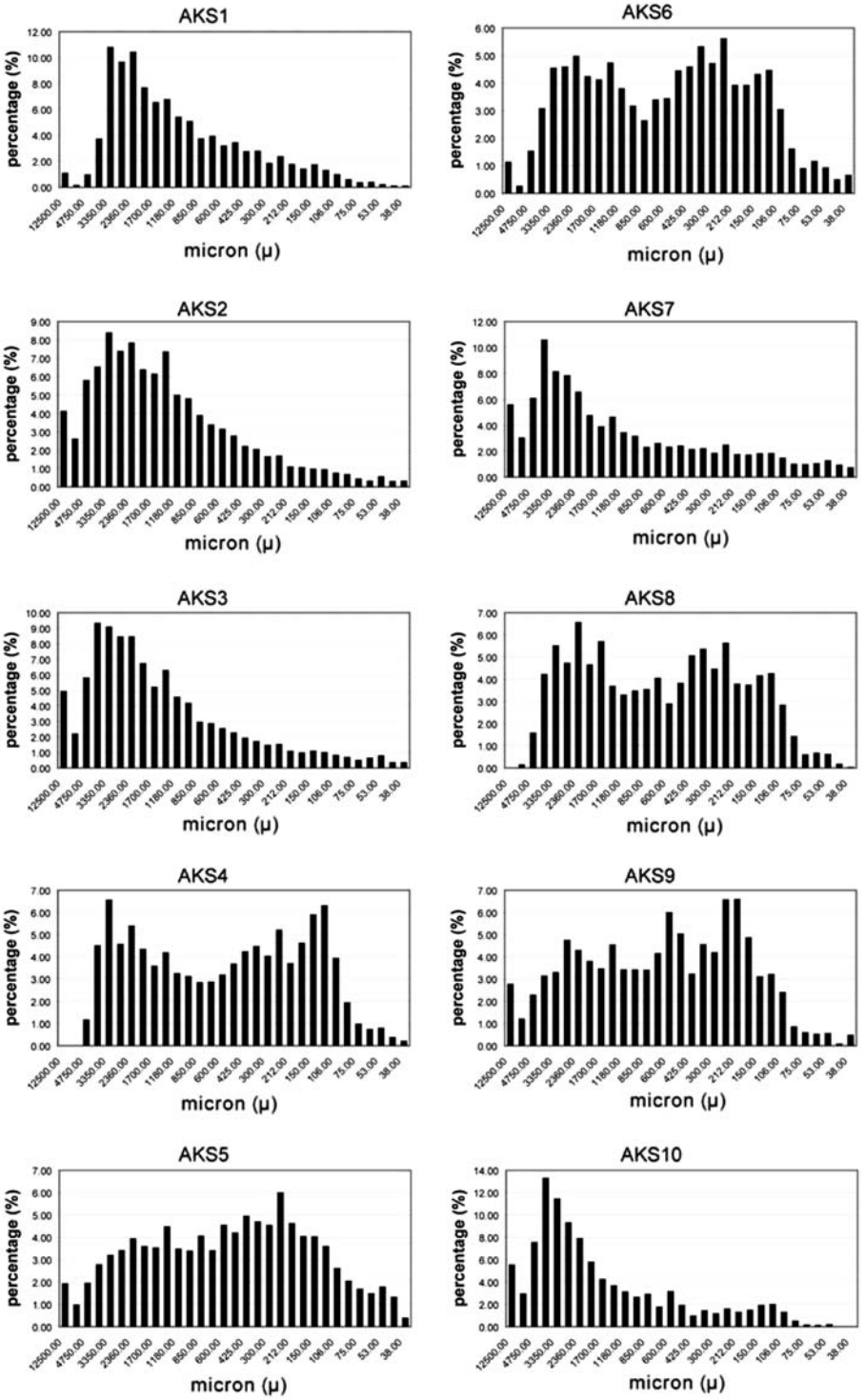

Fig. 8 Grain size distributions shown in histogram form for fresh aggregate samples AKS1–AKS10. Histograms show variation in the modes present

spacings of between 1.78 and 1.88 nm identifies the mineral as a smectite.

Based on visual inspection using TEM imaging, smectite constitutes approximately 90% of the sample volume. Approximately 95% of the particles of smectite have a poorly formed platy to lamellar aggregate texture, similar to that described in Güven (1988). Diameters of these discrete particles of smectite are commonly between 0.1 and 5 μm in length (Fig. 10). The remaining 5% consists of a folded lamella texture. EDS analyses of the smectite (Table 4) are consistent with a Ca-rich montmorillonite, with minor amounts of Fe (assuming Fe^{3+}) and Mg. Both textures have very similar chemical compositions. Some particles have appreciable K content (0.28–0.78 wt% K_2O).

Table 2 Measured coefficients of permeability (K) of fresh aggregate and representative permeability estimations based on grain size distribution

	K value observed	SD	Sheperd		Hazen		Alyamani and Sen	
			1989	Overestimated	1911	Overestimated	1993	Overestimated
AKS1	0.020	0.004	0.039	0.019	2.916	2.896	0.235	0.215
AKS2	0.016	0.002	0.040	0.024	4.356	4.340	0.279	0.263
AKS3	0.025	0.002	0.041	0.016	3.600	3.575	0.396	0.371
AKS4	0.003	0.001	0.031	0.028	0.676	0.673	0.034	0.031
AKS5	0.006	0.002	0.032	0.026	0.576	0.570	0.032	0.026
AKS6	0.027	0.001	0.032	0.005	0.676	0.649	0.035	0.008
AKS7	0.018	0.002	0.041	0.023	0.900	0.882	0.448	0.430
AKS8	0.017	0.004	0.033	0.017	0.900	0.883	0.049	0.032
AKS9	0.009	0.003	0.033	0.023	1.024	1.015	0.039	0.029
AKS10	0.023	0.002	0.042	0.020	3.600	3.577	0.661	0.639
Average	0.016		0.036		1.922		0.221	

Equations used for each estimation are: $K = 100d^{1.5}$ for Sheperd (1989), $K = 40d_{10}^2$ for Hazen (1911), $K = 1300[I_o + 0.025(d_{50} - d_{10})]^2$ for Alyamani and Sen (1993). All values have been converted to cm/s

Table 3 XRF analyses minor and trace elements of fresh aggregate samples and dolomite samples

Sample		Ba (ppm)	Mo (ppm)	Nb (ppm)	Zr (ppm)	Y (ppm)	Sr (ppm)	U (ppm)	Rb (ppm)	Th (ppm)	Pb (ppm)	Zn (ppm)	Cu (ppm)	Ni (ppm)	Co (ppm)	Cr (ppm)	V (ppm)	TiO_2 (%)
AKS	1	4	b.d.	1.4	38	10	603	0.71	b.d.	0.7	4	4	b.d.	b.d.	7	6	b.d.	0.035
AKS	2	13	b.d.	2.1	34	9	541	0.13	b.d.	1.3	3	3	b.d.	b.d.	11	6	b.d.	0.009
AKS	3	8	b.d.	1.6	34	9	542	0.66	b.d.	b.d.	3	3	b.d.	b.d.	4	5	50	0.004
AKS	4	6	b.d.	1.3	intf	8	4004	1.84	b.d.	1.0	3	4	b.d.	b.d.	5	5	b.d.	0.003
AKS	5	7	b.d.	1.4	intf	9	1524	0.63	b.d.	0.7	4	4	b.d.	b.d.	3	4	41	0.003
AKS	6	6	b.d.	1.0	intf	8	3633	0.60	b.d.	0.9	4	3	b.d.	b.d.	1	2	56	0.006
AKS	7	6	b.d.	1.3	38	8	619	0.80	b.d.	1.1	3	3	b.d.	b.d.	3	3	48	0.009
AKS	8	9	b.d.	1.2	intf	8	3724	1.36	b.d.	b.d.	4	4	b.d.	b.d.	11	7	b.d.	0.006
AKS	9	15	b.d.	1.7	intf	8	1470	0.55	b.d.	b.d.	3	4	b.d.	b.d.	3	6	b.d.	0.003
AKS	10	14	b.d.	1.2	36	9	601	1.37	b.d.	0.7	4	3	b.d.	b.d.	2	5	b.d.	0.006
Average		9	b.d.	1	36	9	1726	1	b.d.	1	3	4	b.d.	b.d.	5	5	49	0
REF	1	51	b.d.	0.9	18	8	168	0.03	b.d.	0.7	5	4	b.d.	b.d.	3	18	69	0.0055
REF	2	32	b.d.	1.5	17	7	150	0.71	b.d.	0.6	4	4	b.d.	b.d.	6	16	90	0.0022
REF	3	17	b.d.	1.5	18	8	171	1.24	b.d.	0.3	4	4	b.d.	b.d.	4	15	71	0.0045
REF	4	39	b.d.	2.2	17	8	176	2.77	b.d.	1.1	5	5	b.d.	b.d.	4	14	72	0.0049
REF	5	56	b.d.	1.6	18	7	182	1.51	b.d.	0.3	6	4	b.d.	b.d.	5	17	76	0.0038
Average		39	b.d.	2	17	8	169	1	b.d.	1	5	4	b.d.	b.d.	4	16	76	0

Some K_2O contents of platy to lamellar aggregates are consistent with a R0 (Reichweite, R = 0) interstratified illite–smectite

Kaolinite constitutes approximately 10% of the clay unit volume based on visual estimation from TEM imaging. The texture of kaolinite particles vary from rounded to nearly euhedral (Fig. 10). Diameters of the kaolinite particles vary between 0.80 and 0.01 μm. EDS analyses are consistent with most kaolinites, however, minor amounts of Fe_2O_3 (assuming Fe^{3+}) are present. Imaging indicates that the Fe is a component of kaolinite and not the result of fine-grained Fe-oxide inclusions.

Ti-oxide minerals occur in three textures and compose <1% of the sample volume (Fig. 11). Of these minerals approximately 35% occur as isolated single crystals that are commonly 30–200 nm in diameter and approximately 90% of these grains are euhedral and the remaining 10% are sub-rounded to well-rounded. Another texture that

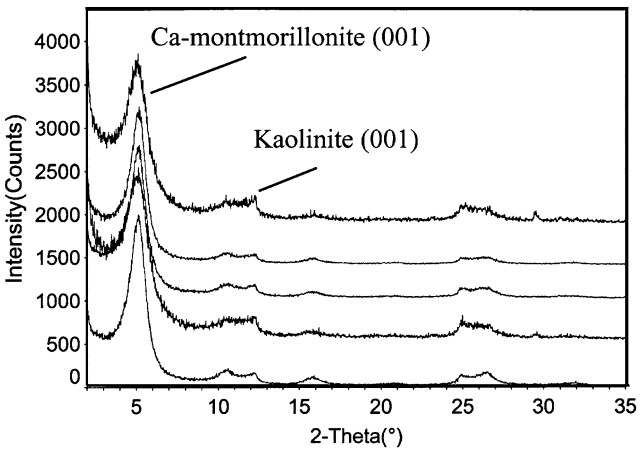

Fig. 9 X-ray diffraction patterns of samples from Mg-exchanged ethylene glycol experiments. Smectite (Ca-montmorillonite) is the dominant mineral as indicated by the large (001) peak. Minor amounts of kaolinite are indicated by the (001) peak

comprises roughly 60% of Ti-oxides is that of larger aggregates that are commonly 0.1–1.0 μm in diameter. Crystals forming these larger aggregates are randomly intergrown, commonly 30–50 nm in diameter, and are euhedral. EDS analyses for both of these textures (Table 4) show that these minerals have some Fe (assuming Fe^{3+}) that varies from 1.90 to 8.75 wt% Fe_2O_3 and also some Zr that varies from 1.79 to 3.05 wt% ZrO_2. The remaining 5% of the Ti-oxide minerals are rectangular laths or prisms which are approximately 0.2 μm wide and 0.5–1.0 μm long. These particles have minor Fe content <2% Fe_2O_3 and no Zr content.

Quartz, aluminosilicate, and apatite are trace minerals identified in the clay. Quartz occurs as sub-rounded to subangular grains 0.5–0.1 μm in diameter. Aluminosilicate occurs as euhedral to subangular rectangular grains and is less common than quartz. Apatite occurs as elongated irregular grains. The approximate ratio of quartz:apatite:aluminosilicate is 10:3:1.

Dolomite

Powder X-ray diffraction indicates that dolomite from Reforma is >99% pure dolomite (Fig. 12). Other mineral phases could not be observed in the diffraction patterns. The most intense reflection for dolomite is (104) with $d_{(104)}$ = 0.288 nm.

Bulk XRF investigation of minor and trace metal concentrations of dolomite samples indicates that there are some heavy metals that are present at ppm concentrations (Table 3). These are Pb (4–6 ppm), Zn (4–5ppm), Co (3–6 ppm) and Cr (15–18 ppm). Concentrations of Mo, Cu, and Ni are all below detection limits (<1 ppm). Ti (0.0022–0.0055 wt% TiO_2) and V (69–90 ppm) are also present.

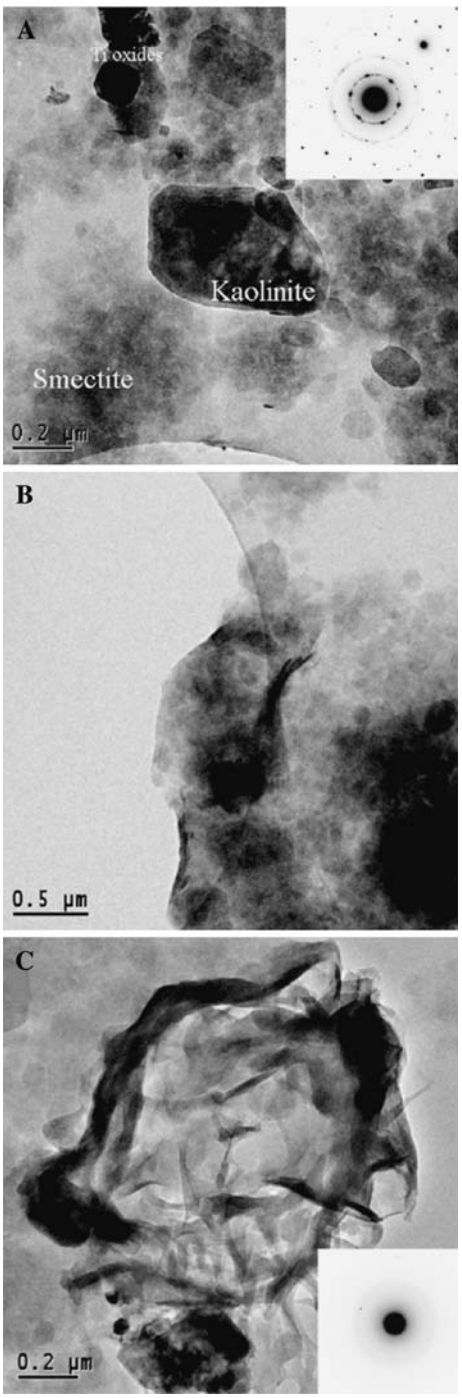

Fig. 10 **a** TEM image showing particles of kaolinite, smectite, and Ti-oxides. **b** TEM image of common textures of aggregates of smectite particles over a hole in carbon film. Particles are platy to lamellar in nature. **c** Example of foliated lamellar texture of smectite that is less common in the unit

Minor elements commonly incorporated into dolomite are also present and are Ba (17–56 ppm), Sr (150–182 ppm), U (0.03–2.77 ppm) and Th (0.3–1.1 ppm). Elements commonly associated with igneous, metamorphic or siliciclas-

Table 4 Representative normalized EDS analyses for Ca-montmorillonite, kaolinite, and Zr-bearing Ti-oxides

Montmorrillonite	1	2	3	4	5	6	7	8
SiO_2	60.71	62.20	61.49	66.94	60.25	59.76	59.06	60.59
TiO_2	0.00	0.00	0.00	0.01	0.00	0.00	0.00	0.00
Al_2O_3	29.41	28.20	28.48	24.52	28.92	28.80	30.37	28.32
Fe_2O_3	4.94	4.03	5.45	3.75	5.54	5.65	4.80	5.46
MgO	2.80	3.67	2.75	3.18	3.03	3.46	2.84	3.84
MnO	0.16	0.04	0.06	0.02	0.00	0.06	0.02	0.00
CaO	1.20	1.49	1.36	1.25	1.85	1.84	1.10	1.31
K_2O	0.78	0.37	0.41	0.33	0.41	0.43	0.28	0.48
Na_2O	0.00	0.00	0.00	0.00	0.00	0.00	1.53	0.00
Total	100.00	100.00	100.00	100.00	100.00	100.00	100.00	100.00

Kaolinite	1	2	3	4	5	6	7	8
SiO_2	54.51	55.54	55.43	54.51	53.42	54.52	54.12	51.78
TiO_2	0.00	0.00	0.00	0.00	0.00	0.00	0.00	0.00
Al_2O_3	42.34	39.07	39.79	42.34	42.78	42.87	41.98	42.47
Fe_2O_3	1.73	3.53	3.29	1.73	2.46	1.34	2.22	4.68
MgO	0.83	1.11	0.91	0.83	0.76	0.81	0.98	0.85
MnO	0.00	0.00	0.00	0.00	0.00	0.00	0.00	0.00
CaO	0.44	0.66	0.47	0.44	0.54	0.38	0.49	0.06
K_2O	0.15	0.09	0.11	0.15	0.04	0.08	0.21	0.16
Na_2O	0.00	0.00	0.00	0.00	0.00	0.00	0.00	0.00
Total	100.00	100.00	100.00	100.00	100.00	100.00	100.00	100.00

Ti-oxide	1	2	3	4	5	6	7	8
TiO_2	91.93	96.17	91.39	89.69	94.59	91.39	88.20	92.93
ZrO_2	2.26	1.93	1.79	2.48	2.73	1.89	3.05	2.99
Fe_2O_3	5.81	1.90	6.82	7.83	2.68	6.72	8.75	4.08
Total	100.00	100.00	100.00	100.00	100.00	100.00	100.00	100.00

tic rocks show low concentrations as expected and are Nb (0.9–2.2 ppm), Zr (17–18 ppm), and Y(7–8 ppm).

SEM investigation indicates that euhedral rhombohedrons which appear to be recrystallized are abundant (Fig. 7). These crystals are commonly 5–15 μm in diameter. The shapes are uniform throughout samples examined. Cracks are occasionally observed within individual crystals. Pores between the crystals compose approximately 10–15% of the rock.

TEM investigation of the insoluble fraction of the Reforma dolomite indicates that goethite and palygorskite are the main impurities (Fig. 13). Goethite crystals are acicular to tabular in morphology. EDS analysis indicate they are pure end member (FeOOH) goethite and selected area electron diffraction (SAED) indicates the goethite crystals are highly crystalline. Size distribution varies from approximately 0.1 to 0.01 μm in length. Palygorskite occurs as fibers approximately 1–3 μm in length and are commonly 0.1–0.05 μm in width. SAED on taken along [hk0] of fibers indicates significant streaking in the *b*-axis direction and have abundant defects in stacking. EDS analysis indicates that chemical compositions of palygorskite fiber are similar to those found in other palygorskite deposits such as those described by Krekeler (2004) and Krekeler et al. (2004).

Discussion

Setting and construction

Some wetlands such as CEA wetland 1 receive loads that exceed original design capacities. The reason for overloaded wetlands is that after installation they are fed extra wastewater, as is the case for CEA wetland 1 which now receives wastewater from a public restroom. Future wetlands in the Akumal area should be designed to receive loads 50% above the current need. By creating a 50%

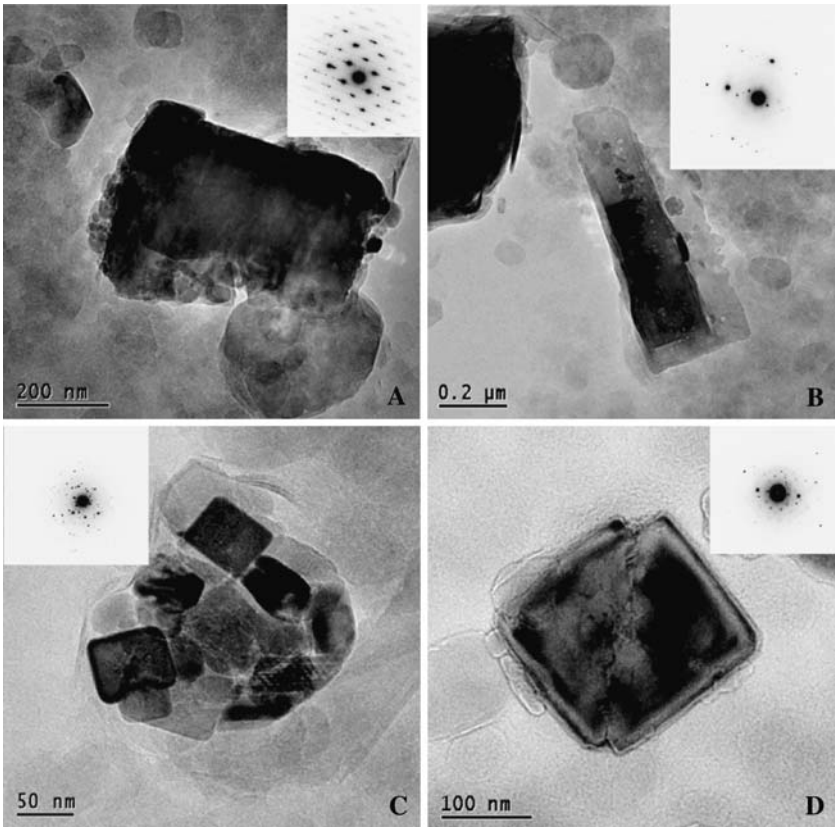

Fig. 11 TEM images of Ti oxide minerals. **a** Equant euhedral grain of Ti-oxide mineral and **b** crystal of rutile. EDS analysis both of these crystals are Ti-rich with minor Fe. **c** Representative of common aggregate of Zr-bearing Ti-oxide minerals. **d** Representative common single grain of Zr-bearing Ti-oxide mineral

buffer capacity this safely allows for expansion of use and may ensure thorough treatment of existing wastewater.

The geometric layouts of the wetland systems in Akumal are variable and some irregularly-shaped systems do not enhance flow. For example ''L'' shaped wetlands and the figure-8 shaped wetland may have regions where water flow is constricted. These configurations cannot be easily retrofitted to enhance performance. Future wetland construction should employ simple rectangular designs with water flow parallel to the long axis of the cells.

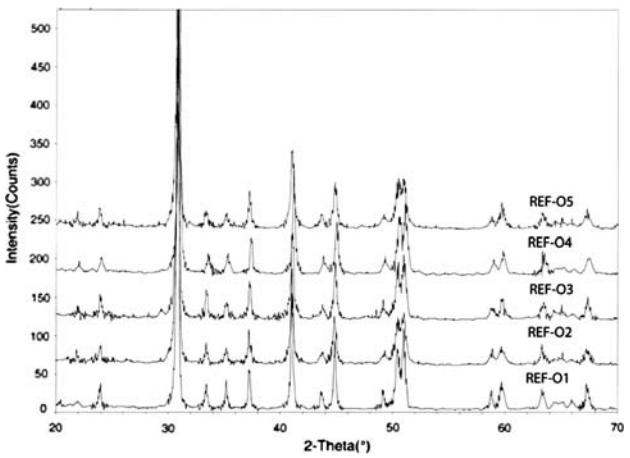

Fig. 12 X-ray diffraction patterns from Reforma dolomite samples REF-O1 through REF-O5. Dolomite is the only mineral that is observed in powder diffraction

Control boxes and clean outs are important features that are present in many of the wetlands of Akumal. In addition to maintenance related use, control boxes and clean outs may be exploited for enhancing or studying the wetlands. Aeration by mechanical or chemical applications could be accomplished via these features of the wetlands. The Las Casitas wetlands are one of the best examples of this because there are redundant and easily accessible control boxes and clean outs in second cells. Retrofitting clean outs may be possible in some wetlands which currently do not have any cleanouts. Because all piping is 4 in. PVC, retrofit technologies may be easily applied and used in multiple wetland systems.

One of the most noticeable and objectionable effects of some constructed wetlands in Akumal is odor. Odor is nuisance but is also a general indication of poor performance. This is of particular concern because some wetlands, such as CEA wetland 1 are located near two outdoor restaurants and odors emitted have potential economic impact for nearby establishments. Odor emission could be reduced in most wetlands by mulching. Currently no systems are purposely mulched, and only three systems have developed a self-mulched layer. Mulching may reduce odor

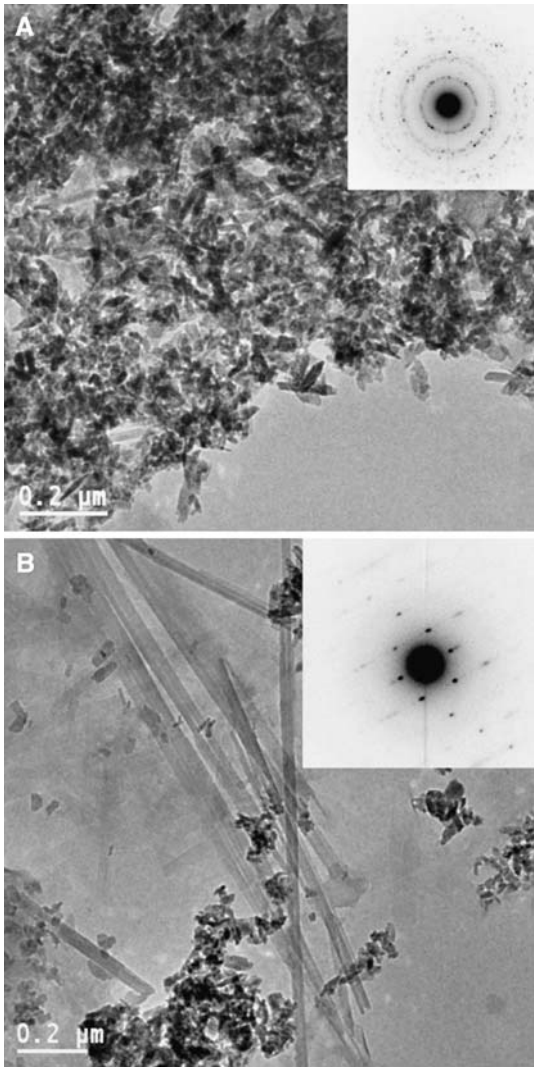

Fig. 13 TEM images of insoluble material from the Reforma Dolomite. **a** shows aggregates of goethite with size distribution of particles being approximately 0.1–0.01 μm in length. **b** shows palygorskite fibers approximately 1–3 μm in length and are commonly 0.1–0.05 μm in width

by creating a low permeability seal and providing sorption surfaces odorous compounds. Sources of mulch are abundant and dead palm tree leaves and other foliage is routinely collected by municipal workers. Using these materials as mulch prevents these materials from being disposed of in local landfills. The use of the Ca-montmorillonite may be a better option because not only will it act as a odor barrier, it may provide a more natural soil structure for the plants. A combination of mulching and using the Ca-montmorillonite may be the best environmental option for odor control.

The observations of plants in the systems have some environmental implications for management. Currently there is little strategy or systematic use of plants in the wetland systems in Akumal. Plant composition in the wetlands is highly variable with the exception being the Las Casitas wetlands. Here these systems are dominated by large ferns that approach 2 m in height and have root systems that penetrate at least 35 cm into the aggregate. These plants clearly thrive in open sun and may be suitable for other wetlands in open sun that currently have poor plant cover.

In the majority of constructed wetlands, plant selection is not optimized for reducing nitrogen compound concentrations in effluent waters. Flowering plants, particularly those that produce fruit take up more nitrogen over simple grasses and non-flowering plants. The use of banana plants is one plant choice that is used in the CEA wetland 1.

Plant choice in the wetlands may also have direct economic impact. Plants grown in wetlands can be used as a renewable resource. Woody plants and certain grasses may be useful for construction materials that are in high demand. Flowering plants may be grown and used as decoration in the local large resorts. Income derived from the sale of these renewable resources could be used to support and improve the wetland systems.

The constructed wetlands appear to be structurally sound. Overall construction could be improved by using geotextile for secondary containment. However, geotextile is not readily available in the region. Secondary containment is of concern because the condition of the bottoms of the wetlands is undetermined and potential exists for corrosion of the bottom. Concrete and mortar that is used in construction of these structures has no appreciable SiO_2 content and the aggregate used is crushed limestone that is soluble in the domestic wastewater interacting with the systems. Another concern regarding the structural integrity of the bottoms of the constructed wetlands is root penetration from trees. Whether or not roots from trees penetrate the bottom concrete slab is undetermined but exists as a potential problem.

Existing aggregate

Aggregate levels in many systems in Akumal have dropped significantly since the time of their construction. We attribute this lowering of aggregate to two processes: compaction and dissolution. Physical inspection of the aggregate in the Akumal systems indicates that dissolution and compaction processes are occurring and mimic natural soil forming processes. Compaction arises from simple settling and also translocation of smaller clasts as shown in Fig. 4. Compaction alone however cannot account for the large volumes of aggregate loss observed in some wetlands. Therefore dissolution must be a major process responsible for the lowering of aggregate levels in these systems. The dissolution of aggregate over the past 6 years

in PCRF supported wetlands has produced drops in aggregate levels from 15 to 60 cm corresponding to rates of dissolution between approximately 3 and 10 cm per year. The continued loss of aggregate will significantly reduce the efficiency of these systems in the near future and the rate of loss of aggregate indicates that some wetlands will be effectively depleted of their aggregate in 6–10 years. This indicates that the effective lifetime of subsurface flow constructed wetlands in Akumal may be on the order of 8 to 10 years before aggregate needs replacement.

Although aggregate levels are currently being depleted causing the efficiency of these systems to degenerate, using limestone as the aggregate in the wetlands may have a benefit. Acids involved in sewage may be neutralized by reactions with calcite and aragonite. Calcite and aragonite are the primary constituents in the limestone of the regional karst aquifer and are currently undergoing dissolution naturally (Tulaczyk 1993). The dissolved cations and anions liberated from aggregate in the subsurface flow wetlands may have minimal impact on the environment as they are already naturally occurring. Therefore the carbonate minerals in the aggregate provide added protection for the environment.

Fresh aggregate

Powder X-ray diffraction investigation of fresh aggregate indicates that some material has as much as 60% aragonite. In both wetlands investigated there was only calcite. This may suggest that if aragonite was present in the wetlands it dissolved preferentially and aragonite is more soluble with Ksp = 8.22 for aragonite and Ksp = 8.35 for calcite (values from Krauskopf 1979). The mineralogy of the fresh aggregate currently used in the systems explains the high degree of aggregate drop. If $CaCO_3$ rich aggregate use is continued, aggregate dominated by calcite should be used preferentially to slow the decrease in reactive volume.

Fresh aggregate samples have permeability coefficients less than that predicted by grain size estimate methods of Hazen (1911), Sheperd (1989), and Alyamani and Sen (1993). Only the method of Sheperd (1989) was within an order of magnitude of observed but consistently overestimated by approximately 50%. This may be corrected by a lower *C* coefficient of 50 instead of 100, but more extensive investigations on other materials are needed to confirm such a relationship. Grain size distributions are both unimodal and multimodal but no clear relationship exists between this property and permeability. The angular nature of the aggregate which arises from crushing combined with the comparatively broad grain size distributions is interpreted as the primary cause for this discrepancy. Intragranular porosity may also play a role as porosity of limestone materials is commonly 10–15%. The results suggest that standard grain size distribution estimations of permeability may be invalid for these particular materials.

XRF investigation reveals the occurrence of Pb, Zn, Co and Cr in both the fresh aggregate samples and the dolomite from the Reforma area. Based on the range of concentrations observed and the rates of aggregate drop an estimate of approximately 0.9–3.0 kg of heavy metals are being released by limestone dissolution in the wetlands studied per year. The fate of these released metals is unclear and whether these metals are having a negative effect on the coral or human health near Akumal is unknown.

Newly discovered geologic resources

The clay unit found in the Reforma region is ideal for a clay liner for the systems. This investigation indicates that there are no minerals that may be damaging to the environment. The only unusual chemical composition was that of the Zr-bearing rutile which is highly insoluble in water at earth surface conditions. The Ca-montmorillonite unit has many properties that make it an ideal choice. Kolstad et al. (2004) found permeability of montmorillonite-rich materials exposed to ionic strengths between 0.05 and 0.5 M are not likely greater than 10^{-7} cm/s. Lee and Schackelford (2005) found that high quality bentonite, primarily defined as high montmorillonite content of 86% had low permeability in $CaCl_2$ solutions. The Reforma clay unit is extremely pure (>95%) Ca-montmorillonite and should behave similarly to montmorillonites investigated by Lee and Schackelford (2005) and Kolstad et al (2004). The Ca^{2+}-rich solution of the wetland systems should not interfere or impede the performance of the clay unit as a liner.

Dolomite from the Reforma region is likely a better aggregate choice because it has a lower solubility (Ksp = 16.54 to 17.09) compared to calcite (Ksp = 8.35) or aragonite (Ksp = 8.22) and has comparatively few impurities (values from Krauskopf, 1979). The fine grain size of the material and the comparatively high porosity is conducive to reacting with wastewater and developing a sustainable microbiota.

Although of small proportion, the impurity minerals of goethite and palygorskite are helpful constituents of the dolomite and are an added benefit compared to the calcite-aragonite aggregate. Goethite for example absorbs a wide range of heavy metals such as Cu, Zn, Pb, Cd, Ni owing to the high proportion of oxygen and the corregated surface structure of the mineral (e.g., Xu et al. 2006; Buerge-Weirich et al. 2002; Christophi and Axe 2000). Goethite has an affinity for sorption of arsenate and phosphate under fresh water to moderately saline conditions (Gao and Mucci 2001) and also for ferricyanide (Rennert and

Mansfeldt 2006). Goethite is the most thermodynamically stable oxyhydroxide at earth surface conditions with $pK_{sp} = \leq 44.1 \pm 0.2$ (Langmuir 1997). Accordingly the presence of goethite in the wetland systems would likely be beneficial as the mineral remains in solid form and absorbs a wide range of potential pollutant metals.

Palygorskite–sepiolite minerals are very reactive and absorbs a wide range of organic compounds and heavy metals (e.g., Shariatmadari et al. 1999, Brigatti et al. 1996). Jones and Galán (1988) proposed three features responsible for the high sorption capacity of palygorskite and sepiolite: (1) Oxygen ions associated with tetrahedra on ribbon edges may attract cations or molecules with dipoles to the mineral surface. (2) H_2O molecules may be coordinated to magnesium ions at the edges of structural ribbons. (3) Silanol groups (–SiOH) occur along the fiber axis of crystals with an estimated density of 4.5 SiOH groups per 100 $Å^2$ for palygorskite and 2.2 SiOH groups per 100 $Å^2$ for sepiolite (Hermosin and Cornejo 1986). Palygorskite is stable in pH values from approximately 7 to 8.5 (Jones and Galán 1988) and thus would likely be beneficial as a component of the wetland system aggregate because it would absorb numerous pollutants.

The Reforma dolomite has comparable heavy metal concentrations to the fresh aggregate; however Cr is higher (14–18 ppm). Heavy metals are likely sorbed onto goethite particles in the dolomite. Aqueous species of Cr are known to sorb on to iron oxides (e.g., He and Traina 2005; Lazaridis et al. 2005; Mineno and Okazaki. 2004). TEM investigation revealed no Cr-rich mineral phase and thus Cr is likely strongly bound to goethite or is mineralized at the trace element level. The low solubility of pure goethite suggests that the Cr, if mineralized poses no significant environmental risk. Cr sorbed to the surface may be retained on goethite in alkaline pH conditions (He and Traina 2005). The Cr that occurs in the dolomite is therefore likely stable.

Conclusions

The constructed wetlands of Akumal represent, to a large extent a success story with much room for improvement. Akumal provides a model where subsurface flow constructed wetlands are effectively used at a community level, however, there are several technical problems with the existing systems. Some problems such as spatial arrangement cannot be remediated while other problems such as geomaterials selection and use can be readily corrected. Future construction of subsurface flow wetlands should follow engineering and scientific guidelines such as those set by Kadlec and Knight (1996) and Reed et al. (1995). By following scientific and engineering guidelines, and implementing the newly discovered geomaterials of this investigation, even more effective systems can be designed and implemented in the future in Akumal and the Eastern Yucatan as a whole. The implementation of new geomaterials may locally improve the health of the Meso-American Reef, and of drinking water resources.

Although subsurface flow constructed wetlands are relatively simple in design, because they rely on natural processes they are in actuality very complex systems. Complicating this is the perturbations humans place on these systems in their regular use. Therefore long term scientific monitoring is needed to better understand the constructed wetlands of Akumal and develop strategies to produce improved wetland systems in the future. Detailed studies of mineralogy, hydrology, wastewater, plant ecology and chemistry are needed to better understand how wetlands operate efficiently over time.

Acknowledgments We thank Centro Ecológico Akumal for support during this study and Dr. Charles Shaw and Kate Robinhawk for valuable discussion and assistance during field work. We also thank A. J. Rossman for discussion.

References

Alyamani MS, Sen Z (1993) Determination of hydraulic conductivity from complete grain size distribution. Groundwater GRWAAP 31(4):551– 555

Boggs S (1995) Principles of sedimentology and stratigraphy. Prentice Hall, Upper Saddle River, NJ

Brady MJ (1974) Sedimentology and depositional history of coastal lagoons, northeastern Quintana Roo, Mexico. Geological Society of America, Annual Meeting, Field Trip Guidebook 2:148–175

Brigatti MF, Medici L, Poppi L (1996) Sepiolite and industrial wastewater purification: removal of Zn^{2+} and Pb^{2+} from aqueous solutions. App Clay Sci 11:43–54

Buerge-Weirich D, Hari R, Xue HE, Behre P, Sigg L (2002) Adsorption of Cu, Cd, and Ni on goethite in the presence of natural groundwater ligands. Environ Sci Technol 36:328–336

Campbell CS, Ogden M (1999) Constructed wetlands in the sustainable landscape. Wiley, New York

Christophi CA, Axe L (2000) Competition of Cd, Cu, and Pb sorbtion on goethite. J Environ Eng-ASCE 126:66–74

Denny P (1997) Implementation of constructed wetlands in developing countries. Water Sci Technol 35:27–34

Gao Y, Mucci A (2001) Acid base reactions, phosphate and arsenate complexation, and their competitive adsorption at the surface of goethite in 0.7 M NaCl. Geochim Cosmochim Acta 65:2361–2378

Gardener T, Côté IM, Gill JA, Grant A, Watkinson A (2003) Longterm region-wide declines in Caribbean corals. Science 301:958–960

Giraldo, E, Zárate E (2000). Removal of hydrogen sulphide BOD from brackish water using vertical flow wetlands in a coastal Caribbean environment. In: Seventh International Conference on Wetland Systems for Water Pollution Control, pp 927– 935

Güven N (1988) Smectites. Hydrous phyllosilicates (exclusive of micas). Rev Miner 19:495–559

Hazen A (1911) Discussion: dams on sand foundations. Trans Am Soc Civ Eng 73:199

He YT, Traina SJ (2005) Cr(VI) reduction and immobilization by magnetite under alkaline pH conditions: the role of passivation. Environ Sci Technol 39:4499–4504

Herrera-Silvera JA, Comin FA, Aranda-Cirerol N, Troccoli L, Capurro L. (2004) Coastal water quality assessment in the Yucatan Peninsula: Management implications. Oce Coast Manage 47:625–639

Hermosin MC, Cornejo J (1986) Methlyation of sepiolite and palygorskite with diazomethane. Clays Clay Miner 34:591–596

Hughes TP, Connell JH (1999). Multiple stressors on coral reefs: a long term perspective. Limonl Oceanogr 44:932–940

Isphording WC (1984) The clays of the Yucatan: a contrast in genesis. In: Singer A, Galan E (eds) Developments in sedimentology 37 palygorskite–sepiolite occurrences, genesis, and uses. Elsevier, New York, pp 59–73

Jones BF, Galán E (1988) Sepiolite and palygorskite hydrous phyllosilicates (exclusive of micas). Rev Miner 19:631–674

Juwarkar AS, Oke B, Juwarkar A, Patnaik S M (1995) Domestic wastewater treatment through constructed wetland in India. Water Sci Technol 32:291–294

Kadlec R, Knight R (1996) Treatment wetlands. CRC Press, Boca Raton, FL

Klein C, Hurlbut CS (1985) Manual of mineralogy (after J. D. Dana), 20th edn. Wiley, New York

Kolstad DC, Benson CH, Tuncer BE (2004) Hydraulic conductivity and swell of nonprehydrated geosynthetic clayliners permeated with inorganic solutions. J Geotech Geoenv Eng 130:1236–1249

Krauskopf KB (1979) Introduction to geochemistry, 2nd edn. McGraw-Hill, New York

Krekeler MPS, Guggenheim S, Rakovan J (2004) A microtexture study of palygorskite-rich sediments from the Hawthorne Formation, southern Georgia by transmission electron microscopy and atomic force microscopy. Clays Clay Miner 52:263–274

Krekeler MPS (2004) Improved constraints on sedimentary environments of palygorskite deposits of the Hawthorne Formation, southern Georgia from a detailed study of a core. Clays Clay Miner 52:253–262

Langmuir D (1997) Aqueous environmental geochemistry. Prentice Hall, Upper Saddle River, NJ

Lazaridis NK Bakoyannakis DN, Deliyanni EA (2005) Chromium (VI) sportive removal from aqueous solutions by nanocrystalline akaganeite. Chemosphere 58:65–73

Lee J, Shackelford CD (2005) Impact of bentonites quality on hydraulic conductivity of geosynthetic clay liners. J Geotech Geoenv Eng 131:64–77

Manios T, Stentiford E, Millner P (2002a) The removal of NH_3–N from primary treated wastewater in subsurface reed beds using different substrates. J Environ Sci Health A-Toxic/Haz Subst Environ Eng 37:297–308

Manios T, Stentiford E, Millner P (2002b) The removal of indicator microorganisims from primary treated wastewater in subsurface reed beds using different substrates. Environ Technol 23:767–774

McKenna SA, Richmond RH, Roos G. (2001) Assessing the effects of sewage on coral reefs: developing techniques to detect stress before coral mortality. B Mar Sci 69:517–523

Mineo T, Okazaki M (2004) adsorption of Cr (VI) ion on synthetic hydrated oxides of iron. Soil Sci Plant Nutr 50:1043–1046

Moore D, Reynolds R (1997) X-ray diffraction and the identification and analysis of clay minerals. Oxford University Press, Oxford

Nelson M (1998) Limestone wetland Mesocosm for recycling saline wastewater in Coastal Yucatan, Mexico. Doctoral Disseration, University of Florida

Okurut TO, van Bruggen J (2000) Distribution and removal of fecal coliform in a constructed wetland in Uganda. In: Seventh International Conference on Wetland Systems for Water Pollution Control, pp 451–458

Pandolfi JM, Jackson JBC, Baron N, Bradbury RH, Guzman HM, Hughes TP, Kappel CV, Micheli F, Ogden JC, Possingham HP, Sala E (2005) Are U.S. Coral Reefs on the slippery slope to slime? Science 307:1725–1726

Pandolfi JM, Bradbury RH, Sala E, Hughes TP, Bjorndal KA, Cooke RG, McArdles D, McClenahan L, Newman MJH, Parades G, Warner RR, Jackson JBC (2003) Global trajectories of the long-term decline of coral reef ecosystems. Science 301:955–957

Panswad T, Chavalparit O (1997) Water quality and occurrences of protozoa and metazoa in two constructed wetlands treating different wastewaters in Thailand. Water Sci Technol 36:183–188

Pennisi E (2002) Survey confirms coral reefs are in peril. Science 297:1622–1623

Reed SC, Crites RW, Middlebrooks EJ (1995) Natural systems for waste management and treatment. McGraw-Hill, New York

Rennert T, Mansfeldt T (2006) J Plant Nutrit Soil Sci- Zeit Pflanz und Boden 169:335–340

Richmond RH (1993) Coral Reefs: present problems and future concerns resulting from anthropogenic disturbance. Am Zool 33:524–536

Sanchez-Gil P, Yanez-Arancibia A, Ramirez-Gordillo J, Day JW, Templet PH (2004) Some socio-economic indicators in the Mexican states of the Gulf of Mexico. Oce Coast Manage 47:581–596

Seidel K (1966) Reinigung von Gewässen durch höhere Pflanzen. Naturwissen 53:289–297

Seidel K (1976) Macrophytes and water purification. In: Tourbier J, Pierson, RW Jr (eds) Biological control of water pollution, Chap. 14. University of Pennsylvannia Press, Philedelphia

Shariatmadari H, Mermut AR, Benke MB (1999) Sorption of selected cationic and neutral organic molecules on palygorskite and sepiolite. Clays Clay Miner 47:44–53

Shaw C (1997) Yal Ku Laggon and North Akumal: quality and movement of groundwater. Centro Ecológico Akumal Report on Recent Studies

Sheperd RG (1989) Correlations of permeability and grain size. Groundwater 27:633–638

Stott R, Jenkins T, Bahgat M, Shalaby I (1999) Capacity of constructed wetlands to remove parasite eggs from wastewaters in Egypt. Water SciTechnol 40:117–123

Tucker ME, Wright VP (1990) Carbonate sedimentology. Blackwell, Oxford

Tulaczyk, SM (1993) Karst geomorphology and hydrogeology of the northeastern Yucatan Penninsula, Mexico. Masters Thesis, Northern Illinois University

Ward WC, Brady MJ (1979) Strandline sedimentation of carbonate grainstones, upper Pleistocene, Yucatan. AAPG Bull 63:362–369

Wetzel RG (2001) Fundamental processes with natural and constructed wetland ecosystems: short term versus long term objectives. Water Sci Technol 44:1–8

Whitney D, Rossman A, Hayden N (2003) Evaluating an existing subsurface-flow constructed wetland in Akumal Mexico. Ecol Eng 20:105–111

Xu Y, Axe L, Yee N, Dyer JA (2006) Bidentate complexation modeling of heavy metal adsorption and competition on goethite. Environ Sci Technol 40:2213–2218